#4771 REVISION 1

Revised January 13, 2014

Original manuscript submitted October 15, 2013

MANTLE-DERIVED GUYANAITE IN A Cr-OMPHACITITE XENOLITH FROM MOSES ROCK DIATREME, UTAH

Daniel J. Schulze

Department of Earth Sciences and Department of Chemical and Physical Sciences, University of Toronto, Mississauga, Ontario, Canada L5L 1C6

Roberta L. Flemming

Department of Earth Sciences, Western University, London, Ontario, Canada N6A 5B7

Patrick H.M. Shepherd

Department of Earth Sciences, Western University, London, Ontario, Canada N6A 5B7

Herwart Helmstaedt

Department of Geological Sciences and Geological Engineering, Queen's University, Kingston, Ontario, Canada K7L 3N6

Abstract

Guyanaite, naturally occurring β-CrOOH, has been identified in a xenolith of Cr-rich omphacitite from the Moses Rock diatreme in the Navajo Volcanic Field of the southwestern United States. It occurs as the dominant phase in small clusters of accessory minerals, intergrown with kosmochlor-rich omphacite, zincian chromite, eskolaite and carmichaelite. The assemblage is interpreted as the result of metasomatism of chromite-bearing serpentinite by slab-derived fluids during subduction of the Farallon Plate in Laramide time. At the time of entrainment of the xenolith, the rock was undergoing prograde metamorphism, with guyanaite dehydrating to eskolaite plus water. This reaction, and the coeval dehydration of the inferred accompanying host serpentinites (which would have been much more volumetrically significant), provided water for hydration of the subcontinental upper mantle, contributing to uplift of the Colorado Plateau. Recognition of guyanaite as a component of a subducted slab supports recent proposals, based on laboratory experiments, that high-pressure polymorphs of common crustal oxy-hydroxide minerals such as boehmite and goethite (i.e.., high-pressure δ-AlOOH and ε-FeOOH) can transport and store water into the upper mantle.

Key words: guyanaite, upper mantle, xenolith, subduction, jade, kosmochlor, carmichaelite, Colorado Plateau

Introduction

Guyanaite, a polymorph of CrOOH, is a rare mineral, previously described from only three locations. It is named for the type locality in Guyana where it occurs as a component of so-called "merumite" pebbles in gold and diamond placer deposits in the Merume River (Milton and Narain, 1969; Milton et al., 1976), intergrown with two other polymorphs of CrOOH (bracewellite and grimaldiite), eskolaite (Cr_2O_3), mcconnellite (CrOOCu), chromian gahnite and gold.

Here we describe guyanaite in a mantle-derived omphacitic clinopyroxenite xenolith from the Moses Rock diatreme in the Navajo Volcanic Field in southeast Utah, USA (Watson, 1967). Its presence in an upper mantle setting is significant, as the synthetic equivalent, β-CrOOH, has recently been shown to be stable to great depths in the mantle (pressures up to at least 13.5 GPa; Jahn et al., 2012) and thus is a potentially significant repository for water in the upper mantle.

Petrography

The sample we studied (#12-97-50) is a xenolith 6 cm in maximum dimension dominated by pale emerald green clinopyroxene with small clots of dark accessory minerals (clots to 2 mm) around which the clinopyroxene is more intensely green in hand sample and in thin section. Fig. 1 is a back-scatter electron (BSE) image of a portion of one of the clusters of accessory minerals. The clusters are dominated by lamellar intergrowths of guyanaite and clinopyroxene. Stringers of eskolaite traverse the guyanaite or occur at the guyanaite-clinopyroxene interfaces. Patches of chromite are interspersed in some of the guyanaite-dominated clusters and consist of lamellar

intergrowths of two texturally different types of chromite, intergrown at the same scale as are the guyanaite and clinopyroxene. In reflected light and BSE images one type of chromite has a "spongy" texture and a darker BSE response due to lower average atomic number and the other appears "clean" and brighter due to a higher average atomic number (Fig. 1). A few grains of carmichaelite (a hydrous titanate mineral) occur in the clusters. Though similar in reflectivity and BSE response to guyanaite, all carmichaelite grains larger than approximately 10 microns have prominent cleavage (Fig. 1).

Mineral Compositions

Minerals were analysed at Queen's University with a JEOL Superprobe, employing standard wavelength dispersive methods and PAP corrections, using a combination of synthetic and natural standards. Representative compositions given in Table 1 (average compositions and standard deviations).

In this sample guyanaite, nominally CrOOH with 89.4 wt% Cr_2O_3, is inhomogeneous (64.0 - 78.0 wt% Cr_2O_3) and contains substantial quantities of Fe_2O_3 (6.6 - 9.3 wt%) and TiO_2 (2.4 - 10.2 wt%) and smaller quantities of MgO (0.4 - 1.8 wt%) and Al_2O_3 (1.3 - 1.6 wt%) as the main impurities. Cr_2O_3 content is negatively correlated with Fe_2O_3 and TiO_2.

Chromite is the only other accessory mineral in this rock that is significantly inhomogeneous, as the two texturally distinct chromite varieties ("clean" and "spongy") are also compositionally distinct from one another, though homogeneous within each group. The darker grains with the "spongy" texture (chromite I) have greater Al_2O_3 and lower Cr_2O_3 (approximately 5.8 and 55.8 wt%, respectively) than do the lighter, "clean" chromites (chromite

II, approximately 1.9 and 64.9 wt%, respectively). Chromite II is more reduced than chromite I ($Fe^{2+}/\Sigma Fe$ = 0.91 and 0.79, respectively, calculated based on stoichiometry and charge balance). Both types have significant zinc contents (ZnO in the range 5.5 - 5.7 wt% ZnO, equivalent to approximately 15 mole % $Zn(Al,Cr,Fe^{3+})_2O_4$).

Carmichaelite is homogeneous, and dominated by TiO_2 (50.9 wt%) and Cr_2O_3 (29.3 wt%) with lesser Fe_2O_3 (9.3 wt%) and minor MgO (1.4 wt%) and Al_2O_3 (2.2 wt%) as significant minor constituents.

Eskolaite is homogeneous, containing approximately 83.6 wt% Cr_2O_3 with substantial Fe_2O_3 (8.1 wt%) and TiO_2 (6.3 wt%) and minor MgO (1.1 wt%) and Al_2O_3 (1.6 wt%).

In the main body of the rock, clinopyroxenes are virtually Cr-free omphacites with end-member compositions of approximately 10-24 mole percent jadeite ($NaAlSi_2O_6$) and minor (7-13%) acmite ($NaFe^{3+}Si_2O_6$). Within, and immediately adjacent to, clusters of accessory minerals, the omphacitic pyroxenes are bright green and enriched in Cr (to 29 mole percent kosmochlor - $NaCrSi_2O_6$). Table 1 includes analyses of omphacite with the highest Cr value, and the two Cr-poor samples with the highest and lowest jadeite components.

Micro X-ray Diffraction of Guyanaite and Associated Minerals

In situ micro X-ray diffraction (μXRD) of a polished thin section and of material from an accessory mineral cluster extracted from the hand specimen was undertaken with a Bruker D8 Discover Micro X-ray diffractometer at Western University using cobalt radiation (Co kα λ = 1.79026 Å), operated at 35 kV and 45 mA. The theta-theta geometry of this instrument allows the sample to remain horizontal and stationary during data collection. A Göbel mirror parallel

optics system with a pinhole collimator snout produced a nominal beam of 100 μm. Target areas were selected using a remote-controlled XYZ sample stage combined with a microscope and laser system and a CCD camera for context images (e.g., Fig. 2a). Two-dimensional XRD data (e.g., Fig. 2b) were collected using a Hi Star detector with General Area Detector Diffraction System (GADDS) in omega scan mode. In this mode, the source and detector were simultaneously rotated clockwise through 9-20 degrees to enable more lattice planes to satisfy Bragg's Law in non-polycrystalline samples. Two 2D images were collected for each target and integrated and merged to produce conventional intensity vs. 2θ plots for mineral identification by comparison with the International Centre for Diffraction Data (ICDD) database (via Bruker's DiffractPLUS EVA evaluation software).

The μXRD data for the clusters of accessory minerals confirm the presence of guyanaite, kosmochlor and chromite plus minor eskolaite and/or carmichaelite (Fig. 2c). Unambiguous identification of the phases is difficult due to the polymineralic nature and fine grain size of the clusters and the considerable overlap of diffraction lines for the various phases (e.g., Fig. 2c). The data best support identification of guyanaite as the CrOOH polymorph present as the lines for guyanaite are a better match for the unknown than are those of bracewellite and grimaldiite (Fig. 2d).

Textural information from the 2D GADDS images (Fig. 2b) show that guyanaite and the kosmochlor-rich omphacite have similar grain sizes. They are relatively coarse-grained crystallites (the data are bright spots as opposed to complete powder rings - see Flemming, 2007). The streaky nature of the bright spots is probably an orientation effect due to the intergrown nature of the kosmochlor-rich omphacite and guyanaite.

Because of the relatively coarse-grained nature of the crystallites, not all of the expected diffraction lines were obtained from any one location, as, even using omega scan mode, not all lattice planes satisfied the diffraction condition. This added additional ambiguity to phase identification. A stack plot of four targets in various orientations accounts for most of the diffraction pattern for guyanaite (Fig. 2c. and 2d.).

Discussion

Guyanaite, identified here by its composition and crystal structure, has only been described previously from three occurrences, all in crustal rocks. The occurrence in "merumite" pebbles (a complex intergrowth of guyanaite, bracewellite, grimaldiite, eskoliate and other minerals) in Guyana was described as having a hydrothermal origin with a possible protolith of volcanic tuff (Milton and Narain, 1969; Milton et al., 1976). Guyanaite from the Outokumpu massive sulfide deposit in Finland is a hydrous alteration product of eskolaite (Vourelainen et al., 1968), apparently also of late-stage hydrothermal origin. Guyanaite was also mentioned as being a component of lateritic alteration at the Omai mine in Guyana (Voicu and Bardot, 2002).

The guyanaite in this study is from a significantly different geologic setting. The omphacitite xenolith in which it occurs is part of a suite of ultramafic xenoliths that includes low-temperature metamorphic rocks such as lawsonite- and phengite-bearing eclogites, Cr-pyrope xenocrysts with inclusions of hydrous minerals as well as hydrated peridotites and pyroxenites containing minerals such as magnesian chlorite, antigorite and pargasite. All of these rock types are clearly of mantle origin (e.g., McGetchin and Silver, 1972; Helmstaedt and Doig, 1975; Smith, 1979, 1995). Xenoliths of omphacite rocks and jadeite clinopyroxenites were interpreted by Helmstaedt and Schulze (1988) as having origins similar to those of jadeite

bodies associated with serpentinites in crustal settings.

As in such jadeitite bodies ("jade"), this sample is essentially monomineralic sodic clinopyroxene (though not as jadeite-rich as classical jades, which typically have >90mole% jadeite component in the pyroxene - Harlow and Sorensen, 2005). Enrichment of clinopyroxene in the kosmochlor component adjacent to the clusters of Cr-rich minerals in our sample is also similar to that occurring around chromite grains in the famous green jades of Myanmar (e.g., Yang, 1984; Shi et al., 2005). In addition, lawsonite eclogites are associated with some jadeite bodies (e.g., in Guatemala - Tsujimori et al., 2006). A significant difference is that the Navajo omphacitites do not contain secondary minerals such as albite and amphibole that are characteristic of retrograde alteration processes that occur during transport of crustal occurrences of jadeitite from their depths of formation in the mantle to Earth's surface (e.g., Harlow and Sorensen, 2005).

The origin of jade bodies in paleo-subduction zone settings (e.g., Myanmar, Guatemala, California) is thought to be due to metasomatic replacement of chromite-bearing serpentinites in the mantle wedge above active subduction zones, or in bodies of serpentinized peridotite of oceanic lithosphere origin dragged down the subduction zone, by fluids rich in Na, Al and Si derived from prograde dehydration reactions in associated subducted slabs (e.g., Harlow and Sorensen, 2005; Shi et al., 2005; Tsujimori and Harlow, 2012). Either scenario may apply to the sample in this study, as serpentinized peridotites from both environments have been proposed to exist in the Navajo mantle xenolith suite (Smith, 2010).

A serpentinite protolith for the omphacitite in our study is consistent with the presence of the chromite-bearing accessory mineral clusters dominated by Cr-rich minerals, but the

177 evolutionary path from chromite to various Cr-rich minerals in the clusters is complex. The
178 peculiar texture of the lamellar intergrowths of guyanaite and kosmochlor-rich clinopyroxene
179 (Fig. 1) is reminiscent of altered spinel group minerals that have undergone exsolution and
180 oxidation resulting in skeletal intergrowths of relict oxides and alteration products (e.g.,
181 Haggerty, 1991). We interpret the accessory mineral clusters as altered Cr-rich spinels that have
182 experienced a similar history, followed by metasomatism by fluids rich in Na, Al and Si. This
183 metasomatism (the "jade-forming" process) ultimately resulted in replacement of the Al-rich
184 chromite lamellae by omphacite and the Cr-rich lamellae by guyanaite. The lamellar
185 intergrowths of two distinctly different chromites in the clusters (Fig. 1) are apparently relicts of
186 an intermediate exsolution stage between fresh chromite and the guyanaite-kosmochlor
187 intergrowths.

188 The relatively large size of the clusters of accessory minerals (to 2 mm) is inconsistent
189 with the protolith of this sample having been a basalt, as was suggested for the
190 phengite/lawsonite-bearing eclogites from these diatremes, in which the pyroxene is also
191 omphacite (e.g., Helmstaedt and Doig, 1975). Chromites in basalts are typically only tens to
192 hundreds of microns in size. The inferred parent spinels to the guyanaite-dominated
193 intergrowths (mm scale) are thus interpreted as phases in serpentinized peridotite in which spinel
194 grains are typically coarser. As spinel-group minerals in serpentinites have higher Zn contents
195 than do primary spinels in fresh peridotites (e.g., Sack and Ghiorso, 1991), the high Zn content
196 of the chromites in our sample is (15 mole% $Zn(Al,Cr,Fe^{3+})_2O_4$ component) consistent with a
197 serpentinite protolith for this rock, as opposed to direct conversion of peridotite to omphacitite
198 by metasomatism.

Although constraints on the conditions of formation of the guyanaite in this sample are few, the equilibration conditions of various other members of the xenolith suite have been estimated using a variety of methods. Estimated pressures of equilibration are in the approximate range 1.5-3.6 GPa and temperatures are in the range 410-800^{o}C (e.g., Helmstaedt and Schulze, 1988; Smith, 1995, 2010, 2013; Wang et al., 1999; Smith et al., 2004).

The textural relationship between the guyanaite and eskolaite (eskolaite is present as thin rims and small stringers within the dominant guyanaite - Fig. 1) is interpreted as indicating that at the time of entrainment as a xenolith, the rock was undergoing prograde metamorphism and guyanaite was in the process of breaking down (dehydrating) to eskolaite plus water. The conditions of guyanaite stability relative to eskolaite + water determined by synthesis experiments (Jahn et al., 2012) can be applied to constrain the conditions of formation of the guyanaite-eskolaite intergrowths (bearing in mind that the experimental data are for end-member CrOOH and the guyanaite in our sample contains considerable Ti and Fe - Table 1). Both data sets (the equilibration conditions for other xenoliths and the data of Jahn et al., 2012) are shown in Fig. 3, as are the estimated equilibration conditions for three phengite-bearing eclogites (Smith et al., 2004). We suggest that a reasonable estimate of conditions of the beginning of the breakdown of guyanaite to eskolaite in this sample is in the range 650-800^{o}C, 2.5-3.5 GPa.

The discovery of eskolaite intergrown with diamond (Logvinova et al., 2008) confirms that eskolaite is also stable to great pressures. There may be a genetic link between the eskolaite formed by prograde metamorphism of guyanaite in our sample and eskolaite associated with diamond.

Carmichaelite, present as a minor constituent of the accessory mineral clusters, has been

221 described previously only as inclusions in Cr-pyrope xenocrysts from the nearby Garnet Ridge
222 diatreme (Wang et al., 1999, 2000), and no data exist that bear on its stability field. Together
223 with other hydrous minerals included in Cr-pyrope xenocrysts (e.g., amphibole, chlorite,
224 titanoclinohumite), it was interpreted as having formed from fluids derived from Proterozoic
225 subduction (e.g., Hunter and Smith, 1981; Smith, 1987; Wang et al., 1999, 2000), with the
226 products encapsulated in garnets in peridotite during prograde metamorphism of subducted
227 oceanic lithosphere and incorporated into the sub-cratonic Colorado Plateau lithospheric mantle.
228 The presence of strong gradients in Fe/Mg ratios in olivine grains also encapsulated in some of
229 the pyrope xenocrysts was interpreted as due to slow cooling of these minerals, consistent with
230 the interpretation that the encapsulated minerals were formed in the Proterozoic. In a re-
231 evaluation of the Cr-pyrope xenocrysts, based on comparison between their olivine inclusions
232 and olivines in hydrous peridotites, Smith (2010) expressed reservations about their Proterozoic
233 heritage. We interpret the carmichaelite in our sample as having been a stable member of the
234 accessory mineral assemblage in the omphacitite in the open system of the upper mantle, actively
235 undergoing prograde metamorphim at the time of entrainment.
236 These two types of occurrences of carmichaelite are not easily explained by a single
237 mode of formation, as should probably be expected given that they are the only two occurrences
238 of this mineral, and both are in xenoliths from the same volcanic field. In contrast to the model
239 of carmichaelite formation in the Proterozoic, we interpret the carmichaelite/guyanaite xenolith
240 as related to subduction of the Farallon Plate, the origin suggested by Helmstaedt and Doig,
241 (1975) for the Navajo phengite- and lawsonite-bearing eclogites. It may have been a component
242 of the oceanic Farallon slab itself, or may have been part of the serpentinized mantle wedge

243 overlying the subducted plate, as suggested for other xenoliths in the Navajo suite (Helmstaedt
244 and Schulze, 1991; Smith, 2010). The textural relationship of the guyanaite and eskolaite is
245 suggestive of dehydration of the guyanaite to eskolaite + water as an ongoing processes at the
246 time of entrainment of the xenolith into the diatreme. At the time of eruption, this reaction was
247 "live", and indicative of prograde metamorphism during heating and increase in pressure that
248 would accompany descent of the Farallon slab (and accompanying fragments of the wedge) into
249 the sub-Colorado Plateau mantle lithosphere. If our interpretation is valid (also see Usui et al.,
250 2003), either the significance of the carmichaelite-bearing pyropes described by Wang et al.
251 (1999, 2000) should be reconsidered, or the only two known occurrences of carmichaelite have
252 distinctly different origins.

253 Both guyanaite and carmichaelite are hydrous minerals and thus potentially important
254 repositories for water in the upper mantle, as well as vehicles for transporting water during
255 subduction, potentially deep into the mantle. They are, however, rare minerals, and their
256 importance in these processes is unclear. In crustal occurrences of jade, host serpentinites are
257 much more volumetrically significant, and we suggest that large volumes of serpentinite was
258 transported along with the omphacitites and also dehydrated. We concur with Smith (2010) who
259 documented prograde metamorphism of antigorite-bearing meta-serpentinites and suggested that
260 water produced by the dehydration of serpentine hydrated the sub-Plateau mantle lithosphere,
261 contributing to uplift of the Colorado Plateau (also see Humphreys et al., 2003).

262

263 Implications

264 Most of the material in the oceanic crust and upper mantle that is subducted into the

mantle at convergent margins disappears from the geologic record. Notable exceptions include slab-derived components of arc magmas (including volatiles) and the intact examples of rocks in high-pressure and ultrahigh-pressure (UHP) metamorphic terranes (e.g., Ernst and Liou, 2008). The ultramafic xenoliths in the diatremes of the Navajo Volcanic Field of the south-western United States appear to be an exception to this situation. The xenoliths of low-temperature eclogite (some of which contain lawsonite and/or phengite) and related rocks have been interpreted as fragments of the subducted Farallon Plate that were plucked from the flat subduction zone in Laramide time (e.g., Helmstaedt and Doig, 1975; Helmstaedt and Schulze, 1988) and returned to Earth's surface without experiencing the alteration and retrograde metamorphsm that is so pervasive in equivalent high-pressure metamorphic rocks preserved at the sites of former convergent margins (e.g., the Franciscan Formation of California).

With its many similarities to jadeite bodies in serpentinites from convergent boundaries in the crust, the guyanaite-bearing jadeite-rich pyroxenite strengthens this connection. The evidence for the prograde reaction guyanaite = eskolaite + water supports the interpretation that the zonation in the garnets of the Navajo eclogite xenoliths is evidence of prograde metamorphism, as would be expected during subduction of the Farallon Plate (e.g., Helmstaedt and Schulze, 1988), although others disagree with this interpretation (e.g., Smith and Zeinteck, 1979). The evidence of a prograde dehydration reaction also supports the suggestion that some of the Navajo hydrous peridotite xenoliths are also prograde metamorphic rocks and the water released on dehydration reactions in these rocks caused hydration and expansion of the subcontinental mantle lithosphere, contributing to the uplift of the Colorado Plateau (Humphreys et al., 2003; Smith, 2010).

The recognition of guyanaite in a mantle setting is perhaps even more important from a global perspective. Low-temperature/pressure oxy-hydroxide minerals such as goethite (FeOOH) and boehmite/diaspore (AlOOH) have recently been shown to have high-pressure polymorphs (e.g., Sano-Furukawa et al., 2009 and references therein) and it has been suggested that such phases, with stability to extraordinarily high pressures (e.g., Sano-Furukawa et al., 2009 demonstrated stability of δ-AlOOH to 34.9 GPa), may transport water deep into the upper mantle. Although guyanaite is rare (we report the fourth occurrence of this mineral), we have shown that it actually exists in mantle rocks, substantiating theories based on experiments (Jahn et al., 2012). The oxy-hydroxides of Al and Fe, which are much more abundant in low-pressure crustal rocks than are the polymorphs of CrOOH, could certainly be important in transporting water to great depths in their ultrahigh-pressure equivalents, and may yet be identified in UHP rocks.

Acknowledgements

We thank Brian Joy, Alison Dias, Yanan Liu and George Kretschman for technical assistance and Tony Mariano for providing additional microprobe standards. We benefited from discussions with Peter Roeder, Doug Smith and Bjorn Mysen and reviews by Nick Sobolev and Roger Mitchell. NSERC is thanked for financial support.

References

Bohlen, S. R., and Boettcher, A.L. (1982) The quartz-coesite transformation: A precise

309 determination and the effects of other components. Journal of Geophysical Research, 87,
310 7073–7078.
311 Chatterjee, N. D., Johannes, W., and Leistner, H. (1984) The system CaO-Al2O3-SiO2-H2O:
312 New phase equilibria data, some calculated phase relations, and their petrological
313 applications. Contributions to Mineralogy and Petrology, 88, 1–13.
314 Ernst, W.G., and Liou, J.G. (2008) High- and ultrahigh-pressure metamorphism: Past results and
315 future prospects. American Mineralogist, 83, 1771-1796.
316 Flemming, L. (2007) Micro X-ray Diffraction (μXRD): A versatile technique for
317 characterization of Earth and planetaryn materials. Canadian Journal of Earth Sciences,
318 44, 1333-1346.
319 Haggerty, S.E. (1991) Oxide textures - A mini-atlas. In Mineralogical Society of
320 America Reviews in Mineralogy, 25, 129-219.
321 Harlow, G.E., and Sorensen, S.S. (2005) Jade (nephrite and jadeitite) and serpentinite:
322 metasomatic connections. International Geology Review, 47, 113–146.
323 Helmstaedt, H., and R. Doig (1975) Eclogite nodules from kimberlite pipes of the Colorado
324 Plateau -- Samples of subducted Franciscan-type oceanic lithosphere. Physics and
325 Chemistry of the Earth, 9, 95–111.
326 Helmstaedt, H., and Schulze, D.J. (1979) Garnet clinopyroxenite - chlorite eclogite transition in
327 a xenolith from Moses Rock: further evidence for metamorphosed ophiolites under
328 the Colorado Plateau. In: F.R. Boyd and H.O.A. Meyer, eds., The Mantle Sample:
329 Inclusions in Kimberlite and Other Volcanics, p. 357–365, AGU, Washington, D.C.
330 Helmstaedt, H., and Schulze, D.J. (1988) Eclogite-facies ultramafic xenoliths from Colorado

Plateau diatreme breccias: Comparison with eclogites in crustal environments, evaluation of the subduction hypothesis, and implications for eclogite xenoliths from diamondiferous kimberlites. In: D.C. Smith, ed., Eclogites and Eclogite-facies Rocks, p. 387-450, Elsevier, New York.

Helmstaedt, H. H., and Schulze, D.J. (1991) Early to mid-Tertiary inverted metamorphic gradient under the Colorado Plateau: Evidence from eclogite xenoliths in ultramafic microbreccias, Navajo volcanic field. Journal of Geophysical Research, 96, 13225–13235.

Humphreys, E., Hessler, E., Dueker, K., Farmer, G.L., Erslev, E., and Atwater, T. (2003) How Laramide-age hydration of North American lithosphere by the Farallon slab controlled subsequent activity in the western United States. International Geology Review, 45, 575-595.

Hunter, W. C., and Smith, D. (1981) Garnet peridotite from Colorado Plateau ultramafic diatremes: Hydrates, carbonates, and comparative geothermometry. Contributions to Mineralogy and Petrology, 76, 312-320.

Jahn, S., Wunder, B., Koch-Muller, M., Tarrieu, L., and Pohle, M. (2012) Pressure-induced hydrogen bond symmetrisation in guyanaite, β-CrOOH: Evidence from spectroscopy and ab initio simulations. European Journal of Mineralogy, 24, 839-850.

Logvinova, A.M, Wirth, R., Sobolev, N.V., Seryotkin, Y.V., Yefimova, E.S., Floss, C., and Taylor, L.A. (2008) Eskolaite associated with diamond from the Udachnaya kimberlite pipe, Yakutia, Russia. American Mineralogist, 93, 685-690.

McGetchin, T. R., and Silver, L.T. (1970) Compositional relations in minerals from kimberlite

and related rocks in the Moses Rock Dike, San Juan County, Utah. American Mineralogist, 55,1738–1771.

Milton, C., and Narain, S. (1969) Merumite occurrence in Guyana. Economic Geology, 64, 910–914.

Milton, C., Appleman, D.E., Appleman, M.H., Chao, E.C.T., Cuttitta, F., Dinnin, E.J., Dwornik, B.L., Ingram, B.L., and Rose Jr., H.J. (1976) Merumite, a complex assemblage of chromium minerals from Guyana. United States Geological Survey Professional Paper, 887, 1–29.

Sack, R.O., and Ghiorso, M.S. (1991) Chromite as a petrogenetic indicator. In Mineralogical Society of American Reviews in Mineralogy 25, pp. 323-353.

Sano-Furukawa, A., Kagi, H., Nagai, T., Nakano, S., Fukura, S., Ushijima, D., Iizuka, R., Ohtani, E., and Yagi, T. (2009) Change in compressibility of δ-AlOOH and δ-AlOOD at high-pressure: A study of isotope effect and hydrogen bond symmetrization. American Mineralogist, 94, 1255-1261.

Shi, G.H., Stockhert, B., and Cui, W.Y. (2005) Kosmochlor and chromian jadeite aggregates from the Myanmar jadeitite area. Mineralogical Magazine, 69, 1059-1075.

Smith, D. (1979) Hydrous minerals and carbonates in peridotite inclusions from theGreen Knobs and Buell Park kimberlitic diatremes on the Colorado Plateau. In: F.R. Boyd and H.O.A. Meyer, eds., The Mantle Sample: Inclusions in Kimberlite and Other Volcanics, p. 345–356, AGU, Washington, D.C.

Smith, D. (1995) Chlorite-rich ultramafic reaction zones in Colorado Plateau xenoliths: Recorders of sub-Moho hydration. Contributions to Mineralogy and Petrology, 121, 185–

200.

Smith, D (1987) Genesis of carbonate in pyrope from ultramafic diatremes on the Colorado Plateau, southwestern United States. Contributions to Mineralogy and Petrology, 97, 389-396.

Smith, D. (2010) Antigorite peridotite, metaserpentinite, and other inclusions within diatremes on the Colorado Plateau, SW USA: Implications for the mantle wedge during low angle subduction. Journal of Petrology, 51, 1355–1379.

Smith, D. (2013) Olivine thermometry and source constraints for mantle fragments in the Navajo Volcanic Field, Colorado Plateau, southwest United States: Implications for the mantle wedge. Geochemistry, Geophysics, Geosystems, 14 (3), doi:10.1002/ggge.20065

Smith, D., and Zeinteck, M. (1979) Mineral chemistry and zoing in eclogite inclusions from the Colorado Plateau. Contributions to Mineralogy and Petrology, 69, 119-131.

Smith, D., Connelly, J.N., Manser, K., Moser, D.E., Housh, T.B., McDowell, F.W., and Mack, L.E. (2004) Evolution of Navajo eclogites and hydration of the mantle wedge below the Colorado Plateau, southwestern United States. Geochemistry Geophysics Geosystems, 5, doi:10.1029/2003GC000675.

Tsujimori, T., and Harlow, G. (2012) Petrogenetic relationships between jadeitite and associated high-pressure and low-temperature metamorphic rocks in worldwide jadeitite localities: A review. European Journal of Mineralogy, 24, 371-390.

Tsujimori, T., Sisson, V.B., Liou, J.G., Harlow, G.E., and Sorensen, S.S. (2006) Petrologic characterization of Guatemalan lawsonite eclogite: Eclogitization of subducted oceanic crust in a cold subduction zone. in B.R. Hacker, W.C. McClelland, J.G. Liou, eds.,

Ultrahigh-pressure metamorphism: Deep continental subduction, Geological Society of America Special Paper, 403, 147–168.

Usui, T., Nakamura, E., Kobayashi, K., Maruyama, S., and Helmstaedt, H.H. (2003) Fate of the subducted Farallon plate inferred from eclogite xenoliths in the Colorado Plateau. Geology, 31, 589-592.

Voicu, G., and Bardot, M. (2002) Geochemical behavior under tropical weathering of the Barama-Mazaruni greenstone belt at Omai gold mine, Guiana. Applied Geochemistry, 17, 321-336.

Vuorelainen, Y., Hakli, T.A., and Kataja, M. (1968) A hydrated oxide of chromium as a pseudomorph after eskolaite, Outokumpu, Finland. Bulletin of the Geological Society of . Finland, 40, 125–129.

Wang, L., Essene, E.J., and Zhang, Y. (1999) Mineral inclusions in pyrope crystals from Garnet Ridge, Arizona, USA: Implications for processes in the upper mantle. Contributions to Mineralogy and Petrology, 135, 164–178.

Wang, L., Rouse, R. C., Essene, E. J., Peacor, D. R., and Zhang, Y. (2000) Carmichaelite, a new hydroxyl-bearing titanate from Garnet Ridge, Arizona. American Mineralogist 85, 792-800.

Watson, K.D. (1967) Kimberlite pipes of northeastern Arizona. In: P.J. Wyllie, ed., Ultramafic and Related Rocks, p. 261-269, Wylie, New York.

Yang, C.M.O. (1984) A terrestrial source of ureyite. American Mineralogist, 69, 1180-1183.

419

420 Figure Captions

421 Figure 1. Backscatter secondary electron image of a portion of a cluster of accessory
422 minerals in sample 12-90-50. Phases labelled are guyanaite (guy), eskolaite (es), carmichaelite
423 (carm) and chromite (cht). These phases are set in a matrix of omphacite that appears very dark
424 grey in this image. The scale bar represents 20 microns.

425 Figure 2. *In situ* μXRD for accessory minerals from clusters in sample 12-90-50. a)
426 context image of polished thin section with target locations of the four μXRD patterns in c and d.
427 The red box represents the area of the BSE image in Fig. 1, b) two-dimensional GADDS images
428 of raw μXRD data; the bright spots indicate larger crystallites and streaks indicate slight
429 dispersion of crystallite orientation likely due to intergrowth of kosmochlor (kos) and guyanaite
430 (guy). The absence of complete Debye rings indicates that these crystallites do not occur in a
431 random distribution but in oriented mineral clusters; c) stack plot of conventional intensity vs. 2θ
432 diffraction patterns for four target locations (areas 1, 2, 5, 7). The best matching mineral phases
433 from the ICDD database are shown as coloured sticks below the patterns; d) stack plot of the
434 same four patterns (areas 1, 2, 5, 7) compared with ICDD patterns for the CrOOH polymorphs
435 guyanaite, bracewellite and grimaldiite. The DIF pattern of carmichaelite in c) was constructed
436 from the data in Wang et al. (2000). (Omega scan collection conditions: Frame 1 - $\theta_1 = 14.5^o$, θ_2
437 $= 18.0^o$, omega = 9, time = 60 minutes; Frame 2 - $\theta_1 = 31.5^o$, $\theta_2 = 40.0^o$, omega = 20, time = 60
438 minutes).

439 Figure 3. Field of likely equilibration conditions of guyanaite-bearing xenolith (rounded
440 rectangle with dark shading). Black dots are estimated equilibration conditions of three phengite

441 eclogites from Smith et al. (2004). Stability field of guyanaite relative to eskolaite + water
442 (region with light shading represents uncertainty) is from Jahn et al. (2012). The quartz (Qz) -
443 coesite (Coes) transition and the reaction lawsonite = zoisite (Zo) + kyanite (Ky) + quartz (Qz) +
444 H_2O are from Bohlen and Boettcher (1982) and Chatterjee et al. (1984), respectively.
445

Table 1. Electron microprobe analyses of minerals in sample 12-97-50, weight percent oxide.

		guyanaite (9)[a]	s.d.[b]	chromite I (12)	s.d.	chromite II (11)	s.d.
	SiO2	0.05	0.01	0.07	0.04	0.04	0.02
	Al2O3	1.44	0.14	5.84	0.57	1.93	0.36
	TiO2	5.46	2.63	0.17	0.05	0.10	0.05
	Cr2O3	72.74	4.45	55.78	0.79	64.93	1.00
	V2O3	0.12	0.04	0.14	0.03	0.05	
	Nb2O5	0.01	0.01	0.02	0.02	0.01	
	Fe2O3[d]	7.75	0.88	7.05	0.66	2.53	0.51
	FeO	nd[e]		24.36	0.21	24.63	0.17
	MnO	0.09	0.02	0.26	0.04	0.26	0.05
	MgO	1.00	0.51	2.06	0.07	1.82	0.06
	NiO	0.30	0.16	0.13	0.03	0.06	0.02
	ZnO	0.02	0.02	5.71	0.27	5.46	0.20
	CaO	0.11	0.03	0.04	0.02	0.05	0.02
	Na2O	nd		nd		nd	
	K2O	nd		nd		nd	
	Total	89.09		100.99		101.64	
formulae normalized to n cations	n =	1		3		3	
	Si4+	0.001		0.002		0.001	
	Al3+	0.024		0.244		0.082	
	Ti4+	0.058		0.005		0.003	
	Cr3+	0.808		1.562		1.847	
	V3+	0.001		0.004		0.001	
	Nb5+	0.000		0.000		0.000	
	Fe3+	0.082		0.190		0.069	
	Fe2+	nd		0.722		0.742	
	Mn2+	0.001		0.008		0.008	
	Mg2+	0.021		0.109		0.098	

	Ni2+		0.003		0.004	0.002
	Zn2+		0.000		0.149	0.145
	Ca2+		0.002		0.002	0.002
	Na+	nd		nd	nd	
	K+	nd		nd	nd	
	Total		1.000		3.000	3.000
Fe2/(Fe2+Fe3) (molar)					0.792	0.914
Fe3:Cr:Al (molar)					0.095:0.783:0.122	0.034:0.924:0.082

[a] Values in parentheses indicate number of analyses used in average

[b] Standard deviation

[c] Abbreviations: jd - jadeite component, ko - kosmochlor component, ac - acmite component

[d] Fe reported as Fe3+ for guyanaite, carmichaelite and eskolaite. Fe2+ and Fe3+ calculated by charge balance for chromite and omphacite

[e] nd - not determined

carmichaelite (5)	s.d.	eskolaite (4)	s.d.	Omphacite highest ko[c](1)	Omphacite highest jd (1)	Omphacite lowest jd (1)
0.10	0.06	0.12	0.05	54.63	56.21	55.55
1.23	0.03	1.56	0.02	3.18	5.56	2.41
50.94	0.17	6.31	0.35	0.03	0.02	0.01
29.27	0.66	83.59	0.60	10.01	0.08	0.07
0.20	0.03	0.13	0.04	nd	nd	nd
0.04	0.01	0.02	0.01	nd	nd	nd
9.30	0.17	8.09	0.10	2.60	2.49	2.45
nd		nd		2.19	3.75	3.20
0.03	0.01	0.14	0.03	0.04	0.04	0.04
1.40	0.06	1.05	0.08	8.79	11.36	13.92
0.16	0.04	0.38	0.03	0.10	0.12	0.14
0.03	0.04	0.03	0.04	nd	nd	nd
0.26	0.10	0.17	0.04	13.07	16.66	20.47
nd		nd		6.60	4.68	2.59
nd		nd		0.00	0.01	0.00
92.95		101.58		101.25	100.98	100.85
1		2		4	4	4
0.001		0.003		1.984	2.010	2.005
0.020		0.045		0.136	0.235	0.102
0.521		0.117		0.001	0.001	0.000
0.315		1.628		0.287	0.002	0.002
0.002		0.003		nd	nd	nd
0.000		0.000		nd	nd	nd
0.106		0.150		0.071	0.067	0.067
nd		nd		0.066	0.112	0.096
0.000		0.003		0.001	0.001	0.001
0.028		0.039		0.476	0.606	0.749

	0.002		0.008		0.003	0.003		0.004
	0.000		0.001	nd	nd	nd		
	0.004		0.005		0.509	0.638		0.791
nd		nd			0.465	0.324		0.182
nd		nd			0.000	0.000		0.000
	1.000		1.000		4.000	4.000		4.000

jd 14	jd 23	jd 10
ko 29	ko 0	ko 0
ac 7	ac 7	ac 7

Fig 1

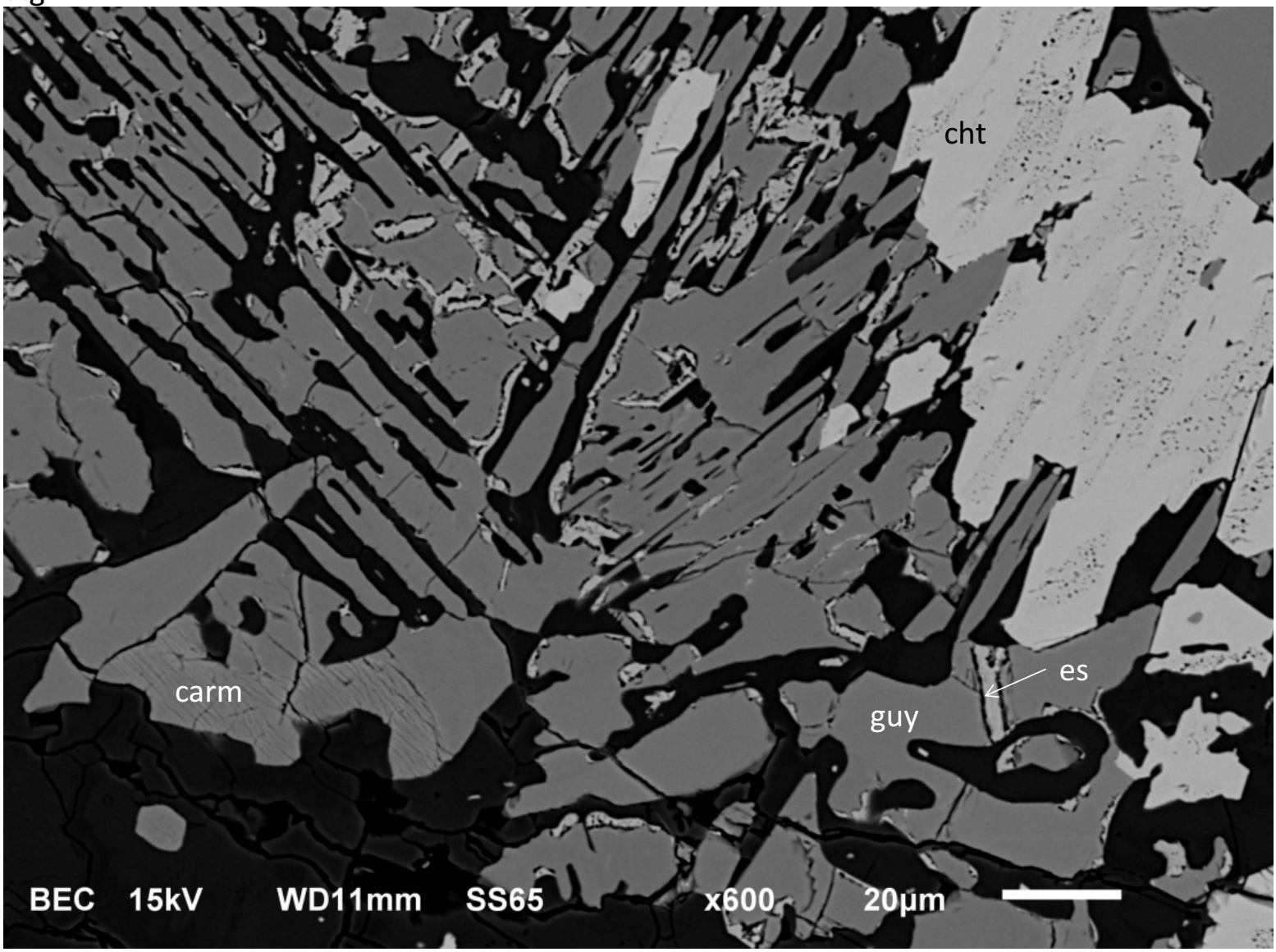

2.a.

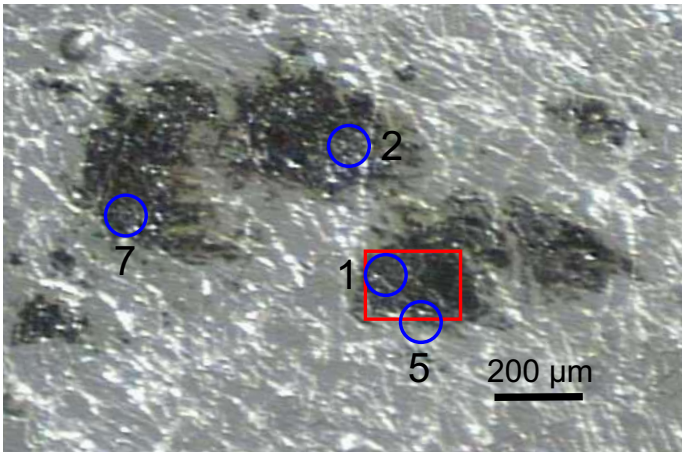

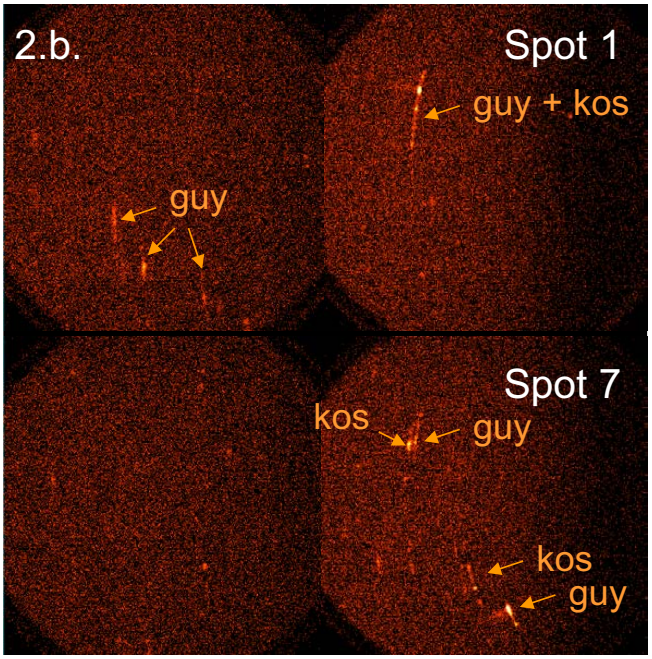

This is a preprint, the final version is subject to change, of the American Mineralogist (MSA)
Cite as Authors (Year) Title. American Mineralogist, in press.
(DOI will not work until issue is live.) DOI: http://dx.doi.org/10.2138/am.2014.4771

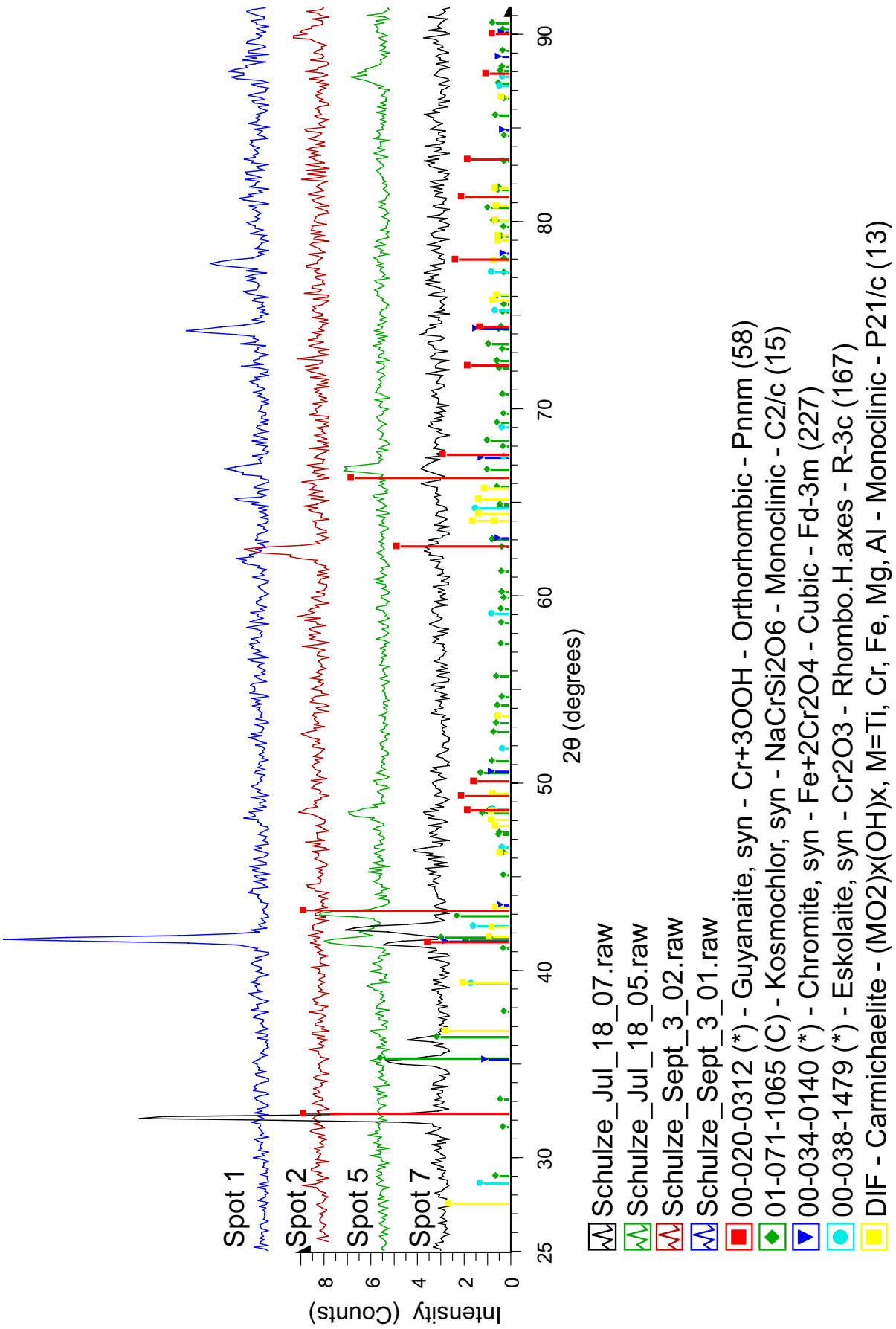

Fig 2.c.

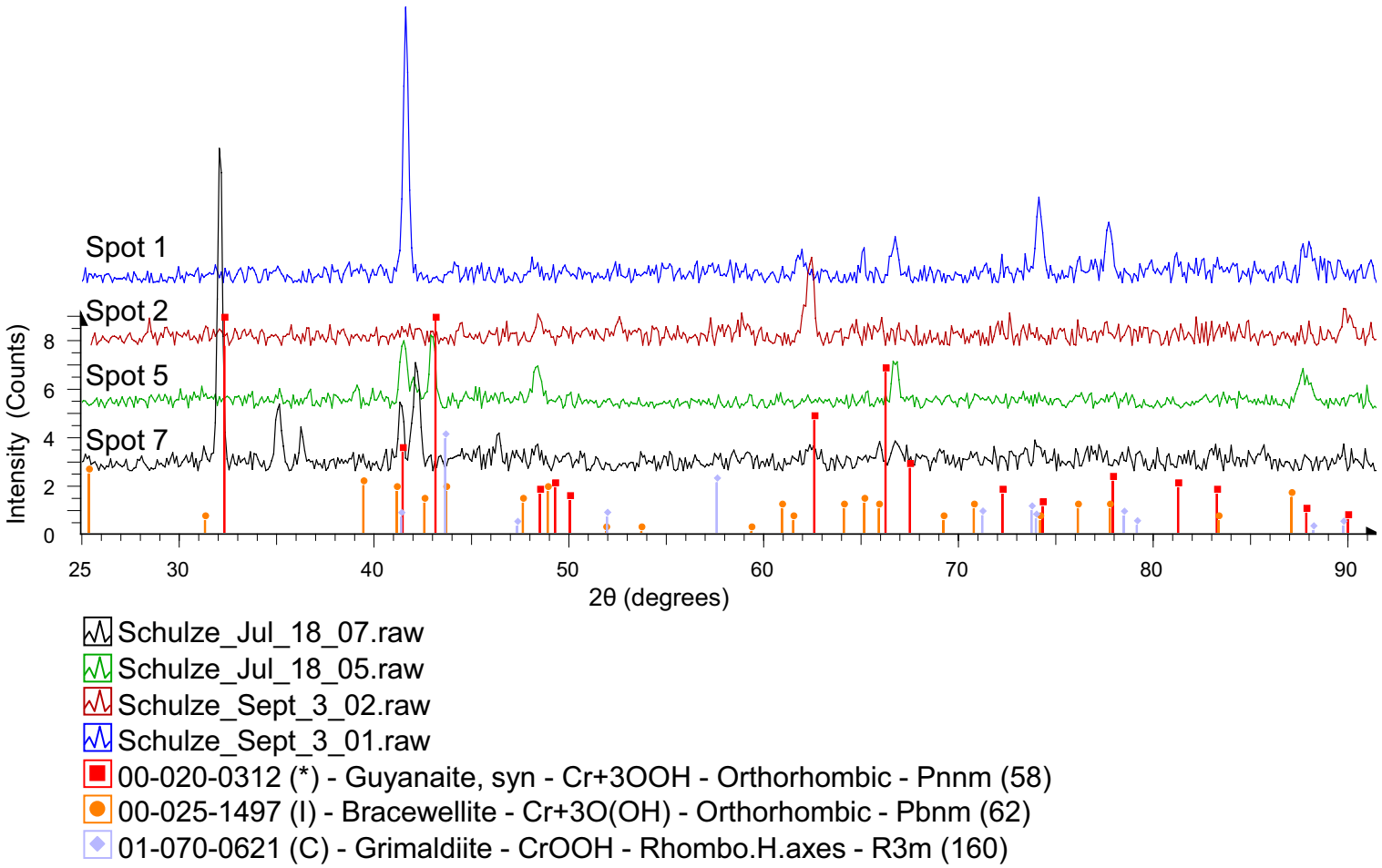

Fig 2.d.

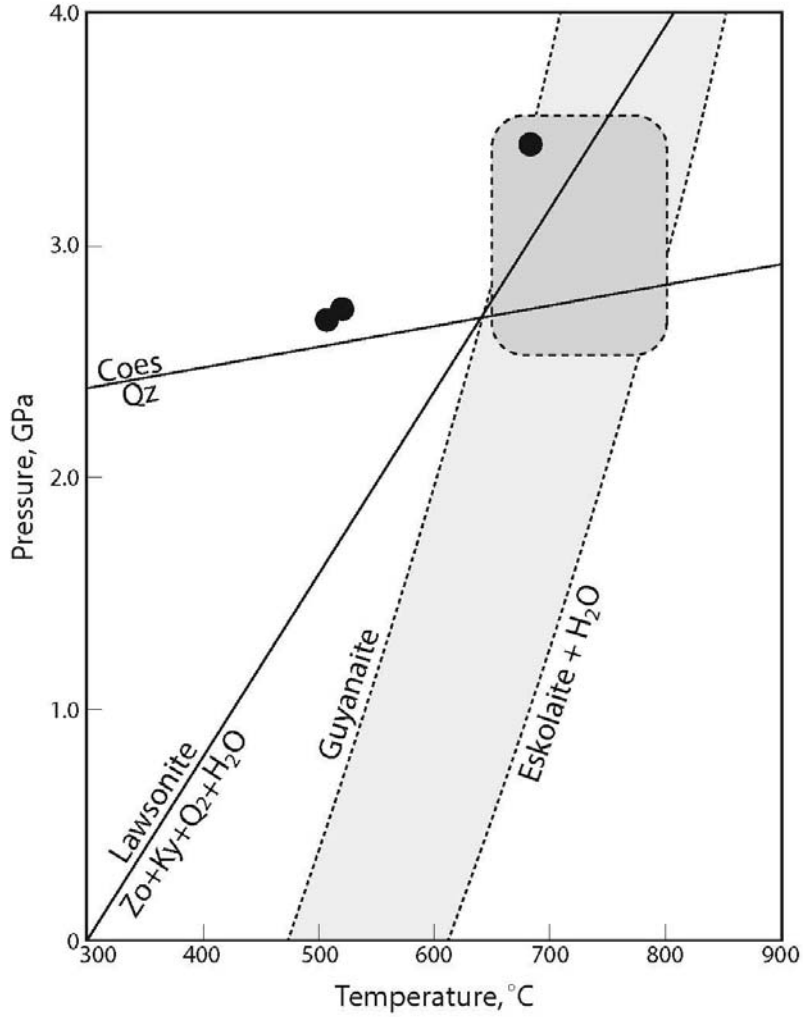
4.0
3.0
2.0
1.0
0
Pressure, GPa
300
400
500
600
700
800
900
Temperature, °C
Coes
Qz
Lawsonite
Zo+Ky+Q2+H2O
Guyanaite
Eskolaite + H2O

Fig. 3